Macromolecules **1985**, *18*, 253–259

Damped Orientational Diffusion Model of Polymer Local, Main Chain Motion. 4. Effects of Probes and Side Chains

Bharat B. Pant, Jeffrey Skolnick,*† and Robert Yaris

Department of Chemistry, Washington University, St. Louis, Missouri 63130.

Received April 2, 1984

ABSTRACT: The complex damped orientational diffusion model of polymer local, main chain motion in moderately dilute solution is extended to include the effects of attached probes and periodic side chains on the dynamics. In the case of an appended probe attached to the main chain, a prescription is given for extracting the contribution of the probe to the local, main chain dynamics and thereby allows one to determine when the probe essentially exerts a minor influence on the character of the local motions and when it does not. In the case of a polymer containing a periodic array of side chains (as is normally the case), we demonstrate that to an excellent approximation in the context of the complex damped orientational diffusion model, side chains merely modify the effective damping constant of an equivalent polymer lacking any side chains. This is an important conclusion that requires experimental verification. Finally, we demonstrate that the complex damped diffusion model in general remains invariant to the particular kind of short-wavelength cutoff employed (either soft or hard) to represent the fact that the fundamental motional unit is of finite extent. In conjunction with the previous conclusion (*Macromolecules* 1982, *15*, 1041) that the model is insensitive to the particular form of the long-wavelength cutoff, this implies a certain robustness of the basic orientational diffusion picture of polymer local motion.

1. Introduction

In a series of papers[1-3] we have developed a damped orientational diffusion model of the local, main chain motion of polymers in solution and have shown that NMR and dielectric relaxation processes can be adequately described by such models. We have also extended the orientational diffusion model to include chain–chain interactions in an averaged way through the use of a complex damping constant,[3] thus enabling it to be applied to more concentrated polymer solutions. In addition, the model has been extended to the case of restricted rotational diffusion.[4] Recently, Viovy, Monnerie, and Brochon[5] presented a detailed comparison of the ability of a variety of diffusional models of polymer local, main chain motion to fit their measured fluorescence depolarization measurements on polystyrene and found that these models fit the measured autocorrelation function very well. It has become increasingly evident as more experimental results are reported and compared to theory that local polymer motion as probed by typical relaxation measurements can be well described by an orientational diffusion picture.

Encouraged by the above, we shall extend the range of applicability of the damped diffusion model of polymer motion to include the effect of spatial inhomogeneties. In particular two cases are explicitly treated. In the first case a polymer chain contains a probe molecule attached to it. Examples include spin-labels required in ESR measurements and dyes required in fluorescence depolarization measurements. Here, we present a procedure for determining whether the probe moiety is essentially benign, that is, it does not change the intrinsic relaxation characteristics of the polymer local motion, and if so, a method is given for extracting the intrinsic motional parameters of the polymer chain. The second case we shall treat is the behavior of a polymer that contains a periodic array of side chains appended to the main chain. Here we shall examine how the power spectrum of the polymer (and hence its relaxation properties) is modified by the presence of the side chains.

In the damped diffusional model, orientational diffusion down the polymer chain is treated as a superposition of damped diffusional waves. In the context of this model an inhomogeneity is treated as an isolated change in the medium (i.e., the polymer chain) through which the diffusional wave is propagating and manifests itself as an isolated local change (increase) in the damping constant of the medium. We further assume that the presence of a probe or side chain does not change the intrinsic short-wavelength, minimum jump time characteristic of the polymer. Support for this assumption has been provided by an examination, via an extension of Kramers rate theory, of the effects of branching (or side chains) on the time scale of the main chain conformational transitions;[6] branches were found to exert a relatively minor effect, and it was concluded that the time scale of conformational transitions in a linear polymer and polymers containing side chains is essentially the same. Hence, we will model the effect of the inhomogeneity as a δ-function with a strength parameter characteristic of the inhomogeneity in the basic diffusion equation.

Another point we shall briefly examine is the demonstration that the results of the diffusional model are largely independent of the precise way in which the small-wavelength cutoff, representing the fact that in a real polymer there is a smallest motional unit, is treated. This is relevant to the understanding of why the various diffusional type models are capable of fitting the experimental data with only minor differences.

The paper is arranged in the following manner: In section 2 the model that includes the effects of inhomogeneities on main chain dynamics is developed. Section 3 develops formal expressions for the autocorrelation function and the power spectrum, which are then solved in section 4 for the case of an isolated side chain and in section 5 for the case of a periodic array of side chains. Finally, in section 6 a brief summary and conclusions are presented. We point out that while this paper is intended to be largely self-contained, it might be helpful for the reader who intends to delve seriously into the derivations to have copies of our earlier papers handy for reference.[1-3]

2. The Model

Let $\rho(x,\hat{e},t)$ be the probability that the bond at position x points along a fixed direction $\hat{e}$ at time t. In the complex damped diffusion model[3] the time evolution of $\rho(x,\hat{e},t)$ is given by a damped diffusion equation

$$\partial\rho/\partial t = [D(\partial^2/\partial x^2) - (\beta + i\gamma)]\rho \qquad (2.1)$$

where x measures the position along the polymer main

---

† Alfred P. Sloan Foundation Fellow.

0024-9297/85/2218-0253$01.50/0

chain and D is the diffusion constant. The damping constant β represents the interaction with the solvent and other polymer chains. The imaginary part of the damping constant, γ, arises from the interaction with other chains.

We now consider the effect of attaching a side chain (or any inhomogeneity) to the backbone at a position x'. In the absence of the side chain, the net orientation at the position x' evolves in two ways. Some of it is propagated to other bonds along the backbone through diffusion and some is lost to the solvent because of the damping. In the spirit of our previous hydrodynamic model of orientational diffusion,[1,3] we now assume that the effect of attaching the side chain is equivalent to a localized change in the medium through which the diffusional wave is propagating. That is, we model the net effect of the side chain as an altered damping constant localized at x'. The extent of this localized damping will, of course, depend on the nature of the appended group and is in general a function of its molecular weight, hydrodynamic properties, bonding structure, etc. It is also possible in principle that the probe or side chain exerts such a drastic influence on the small-scale motion that $D = D(x)$; that is, the intrinsic jump time is position dependent. While it is in principle possible to numerically solve eq 2.1 given a model for $D(x)$ (a nontrivial assumption), we do not believe that this approach would be worthwhile. First of all, the success of the orientational diffusion model as embodied in eq 2.1 depends on the smoothing out of local details. If a $D = D(x)$ is required, it would be more profitable to return to the original finite difference master equation on which eq 2.1 is based.[7] Secondly, if a position-dependent minimum jump time is required to account for a "probe", the appended moiety is examining dynamics that are not representative of the polymer chain in the absence of the probe. Hence, we shall assume that D is a constant independent of whether or not a probe or side chain is appended to the main chain.

Taking the above into account, for a single side chain eq 2.1 becomes

$$\partial\rho/\partial t = [D(\partial^2/\partial x^2) - (\beta + i\gamma) - q\delta(x - x')]\rho \qquad (2.2)$$

where the constant q multiplying the δ-function is the damping constant contributed by the side chain.

One can easily extend eq 2.2 to a periodic array of side chains. For simplicity we shall assume that there is only one kind of side chain in the polymer molecule; thus, all side chains are represented by the same localized damping constant q. The distance between side chains is a. Since the hydrodynamic model only makes sense when the polymer chain is very large compared to the length scale of the local orientational motion (i.e., the chain contour length is very large compared to the damping length), we can for mathematical convenience go to the infinite chain length limit. Thus, the generalization of eq 2.1 to periodic side chains is given by

$$\partial\rho/\partial t = [D(\partial^2/\partial x^2) - (\beta + i\gamma) - q\sum_{l=-\infty}^{\infty}\delta(x - la)]\rho \qquad (2.3)$$

3. Formal Expression for the Autocorrelation Function

In this section we derive a formal expression for the autocorrelation function. In our previous work,[1] by expanding $\rho(x,\hat{e},t)$ in terms of the Legendre polynomials $P_n(\cos\theta)$ where θ is the angle between the instantaneous orientation of the bond vector and the fixed molecular axis z, we demonstrated that all of the normalized autocorrelation functions of rank n are independent of n. Hence, for simplicity we will carry out our analysis using the probability function $\rho(x,t)$, since the final expressions for all normalized tensor autocorrelation functions are identical. In this section we will also treat both the case of a single side chain (described by eq 2.2) and the case of a periodic array of side chains (described by eq 2.3) together by defining

$$V(x) = q\delta(x - x'), \quad \text{single side chain}$$

$$V(x) = q\sum_{l=-\infty}^{+\infty}\delta(x - la), \quad \text{periodic array of side chains} \qquad (3.1)$$

This results in a generalized diffusion equation

$$\partial\rho/\partial t = \{D(\partial^2/\partial x^2) - [\tilde{\beta} + V(x)]\}\rho \qquad (3.2)$$

where

$$\tilde{\beta} = \beta + i\gamma \qquad (3.3)$$

is the complex damping constant.

Decomposing the probability function into a generalized product representation we have

$$\rho(x,t) = \int_k \psi_k(x)\rho_k(t) \qquad (3.4)$$

where we define

$$\int_k \equiv \int_{-\infty}^{\infty} \mathrm{d}k/2\pi \qquad (3.5)$$

for notational convenience. Using the complete orthogonal set of normalized eigenfunctions of the spatial part of the diffusion equation, eq 3.2

$$[\partial^2/\partial x^2 - (1/D)V(x)]\psi_k(x) = -\omega_k^2\psi_k(x) \qquad (3.6)$$

as the expansion function in eq 3.4, we see by inserting the expansion into eq 3.2 that

$$\frac{\mathrm{d}}{\mathrm{d}t}\rho_k(t) = -[D\omega_k^2 + \tilde{\beta}]\rho_k(t) \qquad (3.7)$$

The solution to eq 3.7 is

$$\rho_k(t) = \rho_k(0)e^{-[D\omega_k^2 + \tilde{\beta}]t} \qquad (3.8)$$

where $\rho_k(0)$ is the initial value at time $t = 0$. If we use an impulse condition for our initial condition

$$\rho(0,0) = A\delta(x - x_0) \qquad (3.9)$$

eq 3.4 at 3.8 yield

$$\rho(x,t) = Ae^{-\tilde{\beta}t}\int_k e^{-D\omega_k^2 t}\psi_k^*(x_0)\psi_k(x) \qquad (3.10)$$

Our next step is to calculate the time correlation function $\langle\rho(x,t)\rho^*(x,0)\rangle_x$, where $\langle\,\rangle_x$ denotes the configurational average over the entire length of the chain, L. Moreover, one must incorporate into the time correlation function an a priori probability $P(x_0)\,\mathrm{d}x_0$ that the initial impulse was provided between x_0 and $x_0 + \mathrm{d}x_0$. In our previous work on orientational diffusion[1,3] we did not have to consider such a probability factor *explicitly* due to translational invariance along the polymer backbone. Here, however, owing to the presence of inhomogeneities, we must now explicitly take it into account. When all this is done, we obtain an expression for the normalized time correlation function $\Phi(t)$, given by

$$\Phi(x,t) = \langle\rho(x,t)\rho^*(x,0)\rangle_x/\langle|\rho(x,0)|^2\rangle_x = e^{-\tilde{\beta}t}\int_k e^{-D\omega_k^2 t}g_k(L)\Big/\int_k g_k(L) \qquad (3.11)$$

where we have defined

$$g_k(L) = \int_L \mathrm{d}x_0\, P(x_0)|\psi_k(x_0)|^2 \qquad (3.12)$$

As in our previous work,[1,3] we must introduce an upper cutoff k_m for the wave vector k. The physical origin of the cutoff lies in the inability of a hydrodynamic diffusion model to account for distances shorter than the motional unit which is responsible for the orientational diffusion. Hence, cutting off $1/k$ on the order of the motional unit introduces an upper cutoff k_m. One can equally well interpret the use of an upper wave vector cutoff in a slightly different light. The very use of a diffusion equation to describe the dynamics of local motion implies a slight "smearing out" of motion at the level of a single motional unit since, in reality, such a motion is expected to be discrete. The motion adequately described here is over several motional units. In light of this, one can introduce the upper cutoff k_m at the level of the initial condition given by eq 3.9. If one first expands $\delta(x-x_0)$ in terms of eigenfunctions $\psi_k(x)$ (plane waves in the special case of no side chains) and introduces the upper cutoff k_m, the resulting function is not a δ-function but rather a smeared out distribution of width of $O(1/k_m)$. This is consistent with our picture of local smearing out of the motion. Another way of introducing a cutoff is through the use of a *soft* cutoff function such as $\exp(-k^2/k_m^2)$ inside the integral in eq 3.11. The limit of integration over k is now $(-\infty,\infty)$. Going back to the initial condition, eq 3.9, this choice of cutoff also gives a distribution of width $O(1/k_m)$ instead of a δ-function. Using a straightforward calculation, one can evaluate the correlation function $\Phi(t)$ using the soft cutoff for the special case of no side chains. The functional forms in the limits $t \to 0$ and $t \to \infty$ of $\Phi(t)$ are in agreement (except for a numerical factor) with the calculation done by using a hard cutoff. This discussion about the soft and hard cutoff emphasizes that either choice is ultimately related to the local smearing out of orientational motion. Although we shall use the hard, short-wavelength cutoff in the remainder of this work, one can select either procedure depending upon mathematical convenience. This is very similar to the situation with the long-wavelength (small k) cutoff originally introduced[8] to simulate the effects of damping. This hard cutoff was then replaced with a more physical soft cutoff by introducing the damping constant directly into the diffusion equation.[1] It was shown that the results using the hard and soft cutoff are identical, and one can use either version as a matter of convenience.

At this point one can go no further without explicitly solving the eigenvalue problem eq, 3.6. The solutions are different for the case of an isolated side chain and the case of the periodic array of side chains and so we shall consider these two cases in turn in the next two sections. We shall also obtain the power spectrum, $J(\omega)$ defined by

$$J(\omega) = \mathrm{Re} \int_0^\infty \mathrm{d}t\ e^{i\omega t}\Phi(t) \tag{3.13}$$

4. Isolated Side Chains or Inhomogeneity

In this section we treat explicitly the case of a single side chain or inhomogeneity attached somewhere in the interior of the polymer chain. This corresponds, for example, to a fluorescence or spin-label probe in which the experiment uses the motion of the probe site to infer the motion of the polymer chain. This part of the study aims to develop a formalism which will enable the experimentalist to verify whether a particular probe is benign and, if not, to extract the intrinsic motional parameters of the unperturbed chain.

Using the damped diffusion equation, we model the probe site as a single δ-function located at $x' = 0$ as in eq 2.2. The normalized eigenfunction solutions of eq 3.6 for the single δ-function potential are[9]

$$\Phi_k(x) = e^{ikx} - \frac{is}{2|k|D(k)}e^{i|k|x} \tag{4.1}$$

where

$$D(k) = 1 + is/2|k| \tag{4.2}$$

$$s = q/D \tag{4.3}$$

with the corresponding eigenvalues being given by

$$\omega_k^2 = k^2 \tag{4.4}$$

In evaluating eq 3.11 for the autocorrelation function, note that the orientation is being monitored only at the probe position $x' = 0$; thus, we do not take a configurational average $\langle\rangle_x$. Furthermore, we assume that the probability $P(x_0)$ of the initial impulse, being at position x_0, is distributed uniformly over the chain. Hence

$$P(x_0) = 1/L \tag{4.5}$$

where L is the chain length which is ultimately allowed to go to infinity.

Proceeding in an analogous fashion as in the derivation of eq 3.11 we find that

$$\Phi(t) = \frac{\int_0^{k_m} \mathrm{d}k\ |\psi_k(0)|^2 e^{-Dk^2t}}{\int_0^{k_m} \mathrm{d}k\ |\psi_k(0)|^2} \tag{4.6}$$

Physically $|\psi_k(0)|^2$ is analogous to the transmission coefficient of a plane wave scattered through a single δ-function potential barrier of strength q and accounts for the damping in orientational correlation as the diffusing wave passes through the piece of main chain containing the appended probe. If one explicitly employs eq 4.1 in eq 4.6, it follows that

$$\Phi(t) = \frac{e^{-\beta t}\int_0^1 \mathrm{d}x\ x^2 e^{-x^2\delta t}/(x^2 + \epsilon^2/\delta)}{1 - \dfrac{\epsilon}{\delta^{1/2}} \tan^{-1}(\delta^{1/2}/\epsilon)} \tag{4.7a}$$

where

$$\epsilon = q/(2D^{1/2}) \tag{4.7b}$$

and

$$\delta = Dk_m^2 \tag{4.7c}$$

is the short-wavelength cutoff parameter introduced previously.[1] We have not been able to integrate eq 4.7a exactly, but it is possible to derive an approximation analytic solution of eq 4.7a in the limit

$$\epsilon^2/\delta < 1$$

This is the physically realistic regime where the probe is "benign" and where we would expect the probe to relax on a slower time scale than that of the intrinsic small-scale motion of the polymer chain and to act as a source of orientational damping.

$$\Phi(t) \simeq e^{-\beta t}\left\{\frac{1}{2}\left(\frac{\pi}{\delta t}\right)^{1/2} \mathrm{erf}\,((\delta t)^{1/2}) - \frac{\pi\epsilon}{2\delta^{1/2}}e^{\epsilon^2 t}\,\mathrm{erfc}\,(\epsilon t^{1/2}) + \frac{\epsilon^2}{\delta}[e^{-\delta t} - (\pi\delta t)^{1/2}\,\mathrm{erfc}\,((\delta t)^{1/2})] \middle/ \left[1 - \frac{\epsilon}{\delta}\,\mathrm{sgn}\left(\frac{\epsilon}{\delta^{1/2}}\right)\pi/2 + \epsilon^2/\delta\right]\right\} \tag{4.8}$$

Equation 4.8 may be obtained from eq 4.7 by replacing the integral over k_m in eq 4.6 by an integral from zero to infinity minus the integral from k_m to infinity and expanding the latter integral in powers of ϵ^2/δ. (See ref 1a for a more detailed discussion of the procedure.) We have compared values of $\Phi(t)$ calculated from eq 4.7a with the approximate analytic form, eq 4.8. If $\epsilon/\delta^{1/2} \leq 10^{-1}$, the two expressions agree to four significant figures or better throughout the entire relaxation curve of $\Phi(t)$ vs. t. Even on setting $\epsilon/\delta^{1/2}$ equal to 0.5 (a physically unrealistic value), the approximate and exact forms of $\Phi(t)$ agree to within 4% over the entire course of the decay of $\Phi(t)$ with time. Thus, eq 4.8 can be used with relative confidence.

We should point out that to terms of order ϵ^2/δ, the initial slopes of $\Phi(t)$ vs. t obtained from eq 4.7a and 4.8 agree and are given by

$$\left.\frac{\mathrm{d}\Phi(t)}{\mathrm{d}t}\right|_{t=0} = -\tilde{\beta} - \frac{\delta}{3}\left(1 + \frac{\epsilon\pi}{2\delta^{1/2}} - \frac{4\epsilon^2}{3\delta}\right) \qquad (4.9)$$

Thus, it is not at all surprising that for the physically reasonable regime where $\epsilon/\delta^{1/2} < 1$, the approximate and exact equations for $\Phi(t)$ agree. As is most clearly seen in eq 4.9 for the initial slope, the present model predicts that a probe increases the rate of decay of the orientational correlation function relative to the case of no probe whatsoever. While this might at first appear surprising, in reality it is not. Remember, in the context of the present model, the probe is a localized, structureless entity that acts merely as a sink for orientational diffusion down the main chain and does not change the intrinsic jump time (δ is assumed to be the same with and without the probe).

The power spectrum of eq 4.7a is obtained by inserting $\Phi(t)$ into eq 3.13 to give

$$J(\omega) = [1 - (\epsilon/\delta^{1/2}) \tan^{-1} (\delta^{1/2}/\epsilon)]^{-1}\delta^{-1}\int_0^1 \mathrm{d}x \left[\frac{x^2}{x^2 + \epsilon^2/\delta}\right]\left[\frac{x^2 + \beta/\delta}{(x^2 + \beta/\delta)^2 + (\omega - \gamma)^2/\delta^2}\right] \qquad (4.10)$$

Equation 4.10 can be evaluated analytically, but the results are quite cumbersome. As a practical matter, we retain terms only to lowest order in $\epsilon/\delta^{1/2}$. After a bit of arithmetic, we find

$$J(\omega) = \left\{J_0(\omega) - \left[\frac{\pi\beta}{2\delta^2}(\epsilon/\delta^{1/2}) \operatorname{sgn} (\epsilon/\delta^{1/2})\right]\left[(\beta/\delta)^2 + \frac{(\omega - \gamma)^2}{\delta^2}\right]^{-1}\right\} \Big/ \left\{1 - \frac{\pi\epsilon}{2\delta^{1/2}} \operatorname{sgn} (\epsilon/\delta^{1/2})\right\} \qquad (4.11)$$

where

$$J_0(\omega) = \delta^{-1}\int_0^1 \mathrm{d}x \, \frac{x^2 + \beta/\delta}{(x^2 + \beta/\delta)^2 + (\omega - \gamma)^2/\delta^2} \qquad (4.12)$$

$J_o(\omega)$ is the power spectrum for the complex damped orientational diffusion model[3] without side chains. An exact analytic expression for $J_0(\omega)$ is given by eq II-6 of ref 3.

Equation 4.8 or 4.11 for the autocorrelation function and spectral density, respectively, can be used to analyze experimental data in the following way:

(i) To avoid complications experiments should be done in the dilute-solution regime so that the chain–chain interactions and hence γ are negligible.

(ii) Analyze the relaxation data using the autocorrelation function or power spectrum calculated from the orientational diffusion model without side chains of ref 1 and obtain values of δ and β employing some criteria for the goodness of fit (e.g., a sum of residuals). That is, one first fits to a model which assumes a completely benign probe by neglecting its existence.

(iii) Then refit the relaxation data using the autocorrelation function given in eq 4.8 or power spectrum given in eq 4.11 and obtain new values of δ, β as well as a value for ϵ and the goodness of fit parameter. If the goodness of fit parameter is not appreciably improved over that obtained in step iii (remembering that a three-parameter fit should always be somewhat better than a two-parameter fit) and if the values of β and δ are not changed appreciably from those obtained in step ii, one has then demonstrated (within this hydrodynamic approach) that the probe is acting in a benign fashion in that the intrinsic character of the local motion has remained unchanged.

(iv) If the fit in step iii is reasonably different from what it was in step ii, then the proper diffusional parameters to describe the motion of the chain corrected for the influence of the probe are those from step iii.

(v) If the fit in step iii is still very bad, then either one is looking only at the properties of the probe and not the polymer, and/or the hydrodynamic approach cannot be used to analyze the relaxation data.

5. Periodic Array of Side Chains

A. Mathematical Treatment. We now turn to the case of a periodic array of side chains modeled by a periodic array of δ-functions. The eigenvalue equation for this potential (eq 3.6) is isomorphic to a well-known model for electrons in a solid, the "Kronig–Penney model", and the details of the derivation of the solution for the eigenvectors and eigenvalues can be found in the extensive solid-state physics literature on the subject.[10-13] Hence, we shall only present those features of the eigenstates which are relevant to the present problem.

An immediate consequence of the periodicity of the potential is that the eigenfunction $\psi_k(x)$ must satisfy Bloch's theorem,[12,13] namely

$$\psi_k(x) = e^{ikx}\phi_k(x) \qquad (5.1)$$

where $\varphi_k(x)$ has the periodicity of the potential (i.e., a). A consequence of Bloch's theorem is that the eigenvalue spectrum splits into bands with these bands separated by band gaps. In Figure 1 we have plotted the eigenvalue spectrum as a function of k for a positive value of s' ($=sa$) (a repulsive δ-function potential) equal to 4.5. Such a banded spectrum will be produced for all positive values of s. Note in particular that there is a band gap at $k = 0$, a feature which will be of major importance in the following analysis. The upper band edges are at $k = \pm n\pi$, $n = 1, 2, \ldots$. The band with its upper band edge at $k = \pm n\pi$ is referred to as the nth band.

Another consequence of Bloch's theorem is that there is not a unique labeling of the states $\psi_k(x)$ (see standard references in solid-state physics, e.g., ref 12 and 13). We shall employ the "extended zone scheme"[12] of labeling which restricts the value $(n - 1)\pi \leq |ka| < n\pi$ to correspond to $(n - 1)^2\pi^2 \leq (\omega_k a)^2 < (n\pi)^2$ ($n = 1, 2, \ldots$). This scheme has the advantage that the eigenvalue spectrum simply reduces to the plane wave spectrum $\omega_k^2 = k^2$ as the periodic potential vanishes. Figure 1 was plotted by using this labeling scheme.

The eigenvalues ω_k^2 are obtained as the solution to the transcendental equation[10,11]

$$\cos (ka) = \cos (\omega_k a) + \frac{s}{2\omega_k} \sin (\omega_k a) \qquad (5.2)$$

Since for any nonzero values of s the right-hand side of

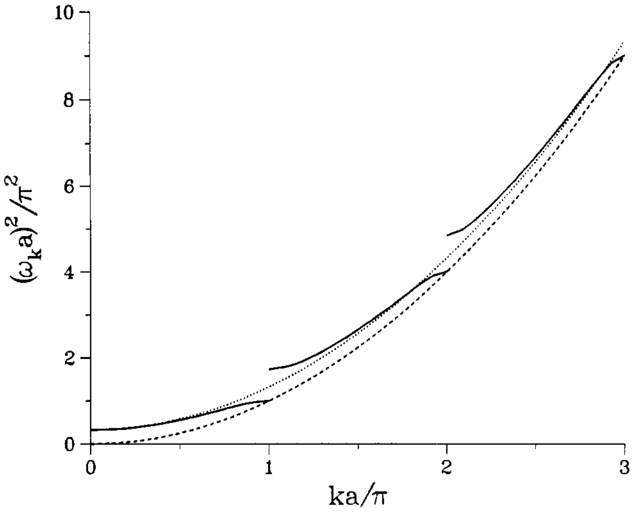

Figure 1. The solid line represents a plot of ω_k^2, the eigenvalue of the spatial part of the diffusion equation (eq 3.2), as determined from eq 5.2, vs. wave vector k for a main chain containing a periodic array of side chains with $s' = 4.5$. The dashed curve is the dispersion reaction, ω_k^2 vs. k for the limiting case of no side chains. The dotted curve is a plot of ω_k^2 vs. k employing the effective damping approximation, eq 5.13.

eq 5.2 can exceed unity while the left-hand side cannot, there are band gaps for certain real values of k. As mentioned above the upper band edges occur at

$$ka = \pm n\pi, \qquad (\omega_k a)^2 = (n\pi)^2; \qquad n = 1, 2, ... \tag{5.3}$$

while the lower band edges are solutions to

$$(\omega_k a/2) \tan (\omega_k a/2) = sa/4, \quad (n \text{ odd}) \tag{5.4a}$$

$$(\omega_k a/2) \cot (\omega_k a/2) = -sa/4, \quad (n \text{ even}) \tag{5.4b}$$

From eq 5.4 one can readily compute the lower band edges numerically.

One can easily obtain the small and large s limiting cases of eq 5.4. To obtain the small s limit of the lower band edges, one expands eq 5.4 as a series in s and obtains

$$\begin{aligned}(\omega_k a)_n^2 &= sa(1 - sa/12 + ...), \quad n = 1 \\ &= (n-1)^2\pi^2 + 2sa + ..., \quad n = 2, 3, ...\end{aligned} \tag{5.5}$$

From eq 5.5 and 5.3 it is readily apparent that band gaps disappear in the limit $s \rightarrow 0$. The lower band edges in the limit $s \rightarrow \infty$ are

$$(\omega_k a)^2 = (n\pi)^2, \quad n = 1, 2, ... \tag{5.6}$$

which coincide with the upper band edges. In this limit the band structure collapses to the discrete level structure of a particle in a box of width a. Since the eigenfunctions are well-known, we shall not reproduce them here (see ref 10 and 11 for the explicit eigenfunctions). One should note that in this limit all of the eigenfunctions have nodes at the positions of the δ-functions.

In order to evaluate the autocorrelation function eq 3.11 for the array of side chains we must first evaluate $g_k(L)$ given by eq 3.12. Again assuming equal a priori probability that the initial impulse, $P(x_0)$, is randomly distributed over the chain (as expressed in eq 4.5) and using the normalization of the eigenfunctions we obtain

$$g_k(L) = 1/L \tag{5.7}$$

independent of k. Using eq 5.7 in eq 3.11 and invoking the hard cutoff k_{m} (see discussion following eq 3.12), we find

$$\Phi(t) = k_{\mathrm{m}}^{-1} e^{-\tilde{\beta} t} \int_0^{k_{\mathrm{m}}} \mathrm{d}k \; e^{-D\omega_k^2 t} \tag{5.8}$$

where the integration is only over positive values of k since ω_k^2 is an even function of k.

Using eq 5.8 in eq 3.13 yields

$$J(\omega) = k_{\mathrm{m}}^{-1} \int_0^{k_{\mathrm{m}}} \mathrm{d}k \, \frac{D\omega_k^2 + \beta}{(D\omega_k^2 + \beta)^2 + (\omega - \gamma)^2} \tag{5.9}$$

It is convenient to replace the wave vector cutoff by

$$k_{\mathrm{m}} = M\pi/a \tag{5.10a}$$

The rationale behind this replacement is that π/k_{m} is the short-wavelength cutoff which physically represents the smallest motional unit. In the simplest visualization of this we consider π/k_{m} a "bond length" and the side chain repeat distance a as an integral multiple of this bond length. In this case M is an integer and the k integration in eq 5.10 becomes an integration over the first M bands. In general, M need not be an integer and then the integration is over a fractional number of bands. For simplicity, in the explicit calculations to be discussed below, we shall use integral values of M; however, the essential results would remain unchanged for nonintegral values of M. We shall also scale the rest of our variables with a by defining

$$k' \equiv ka \tag{5.10b}$$

$$\omega_k' \equiv \omega_k a \tag{5.10c}$$

$$s' \equiv sa \equiv 2\epsilon(M\pi)/\delta^{1/2} \tag{5.10d}$$

with ϵ defined in eq 4.7b. Using these reduced variables, eq 5.9 becomes

$$J(\omega) = (\pi M/\delta) \int_0^{\pi M} \mathrm{d}k' \, \frac{\omega_k'^2 + \frac{\beta}{\delta}(\pi M)^2}{\left[\omega_k'^2 + \frac{\beta}{\delta}(\pi M)^2\right]^2 + \frac{(\omega - \gamma)^2(\pi M)^4}{\delta^2}} \tag{5.11}$$

where δ is given by eq 4.7c.

For the limiting case of a weak side chain interaction, $s \rightarrow 0$, $\omega_k^2 \rightarrow k'^2$ and it is easily seen that eq 5.11 reduces to the power spectrum in the absence of side chains, $J_0(\omega)$ (eq 4.10), as obtained in our previous work.[3] For the other limiting case of strong side chain interaction, $s \rightarrow \infty$, the band structure collapses to the discrete spectrum of eq 5.6 and the power spectrum reduces to a sum

$$J(\omega) = \frac{M\pi^2}{\delta} \sum_{j=1}^{M} \frac{(j\pi)^2 + \frac{\beta}{\delta}(\pi M)^2}{\left[(j\pi)^2 + \frac{\beta}{\delta}(M\pi)^2\right]^2 + \frac{(\omega - \gamma)^2(M\pi)^4}{\delta^2}} \tag{5.12}$$

This strong interaction limit is a sum of Lorentzians with the $j = 1$ term corresponding to the most slowly decaying mode. In this limit, all of the orientational decay occurs between a pair of side chains since there is an infinitely high potential barrier at the location of each side chain; i.e., the diffusing mode behaves like a quantum-mechanical particle in a box. Of course, if the side chains' repeat distance is large compared to the damping length, the major contribution to the dynamics becomes the damping in the absence of side chains, and the power spectrum reduces to the case of no side chains, $J_0(\omega)$. This can be shown even in the case of $s' \rightarrow \infty$ since as $a \rightarrow \infty$, $M \rightarrow \infty$ and eq 5.12 is a series representation of $J_0(\omega)$.

B. Numerical Evaluation of the Power Spectrum. Before proceeding with the evaluation of $J(\omega)$ we must first discuss reasonable ranges of values of the parameters. As

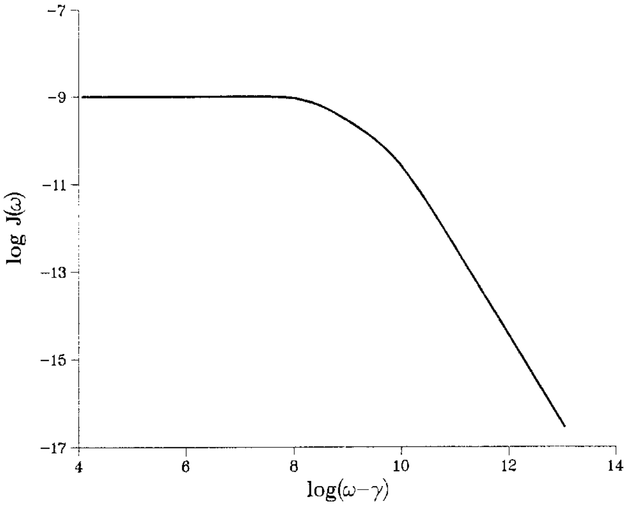

Figure 2. Representative plot of log ($J(\omega)$) determined via eq 5.11 vs. log ($\omega - \gamma$) employing $\beta/\delta = 0.01$, $s' = 1.0$, and $M = 3$.

explained at the end of the previous subsection, if the distance between side chains becomes large relative to the damping length, then the presence of side chains becomes irrelevant. Hence, for real polymer chains we can consider M to be in the range of 1–10 units between side chains. Plausible values of β and δ can be obtained from our previous work[2] where we fit the experimental values of NMR relaxation rates of poly(vinyl acetate) and we found a value of $\beta/\delta \sim O(10^{-2})$. While ultimately the strength of the side chain interaction parameter, $Ds/a\delta = 2\epsilon/M\pi\delta^{1/2}$, will have to be experimentally determined, one would not reasonably expect it to be more than 1 order of magnitude greater than β/δ. The chain–chain interaction parameter, γ, serves only to shift the frequency in the power spectrum (see eq 5.9 or 5.11), so we calculate the power spectrum as a function of the shifted frequency ($\omega - \gamma$).

The power spectrum was evaluated by first numerically solving the transcendental equations (5.4) for the lower band edges. Knowing these, one can then solve for ω_k' as a function of k' within the given band. We then integrated eq 5.11 numerically using the known band structure to obtain $J(\omega)$. We have performed these calculations over a wide range of representation parameters. The value of β/δ was varied from 10^{-5} to 1 and $s' = 2M\pi\epsilon/\delta^{1/2}$ was varied from 10^{-3} to 10^{6} and M was taken to be 1, 3, and 6. We have plotted a representative example of the calculated power spectrum in Figure 2.

Before we discuss the numerical results, note that for $Ds/a\delta$ of the order of β/δ the dominant contribution to the integral in eq 5.11 comes from the region where $k' \simeq 0$. Thus, for small values of s' we can approximate the eigenvalue spectrum by a shifted parabola

$$\omega_k^2 = k^2 + \omega_0^2 \tag{5.13}$$

where ω_0^2 is the lowest band gap (i.e., the value of ω_k at the bottom of the first band—see Figure 1). The value of ω_0 is easily calculated numerically by using eq 5.4a and in the limit that $s \to 0$, $\omega_0^2 = s/a$. In fact, within 10%, ω_0^2 is given by s/a for all reasonable values of s, i.e., s' on the order of unity. Inserting eq 5.13 into eq 5.9 we obtain

$$J(\omega) = \delta^{-1}\int_0^1 \mathrm{d}z\, \frac{z^2 + (\beta + D\omega_0^2)/\delta}{[z^2 + (\beta + D\omega_0^2)/\delta]^2 + (\omega - \gamma)^2/\delta^2} \tag{5.14}$$

As we can see by comparing eq 5.14 to eq 4.12 that this is the identical power spectrum obtained in the absence of side chains, $J_0(\omega)$, except that the damping constant β has been replaced by an effective damping constant $\beta + D\omega_0^2$ (approximately equal to $\beta + (2\epsilon\delta^{1/2})/M\pi$). This effective damping constant takes into account the presence of the side chains. It would at first glance seem that replacing the rich band structure of the eigenvalue spectrum depicted in Figure 1 by the simpler dispersion relation of eq 5.13 would be a gross oversimplification. However, one must realize that the power spectrum is an integral over the band structure. By looking at Figure 1 where the simple dispersion relation eq, 5.13 is also plotted, one can see that what one loses from the integral at the top of a band one approximately makes up at the bottom of the next band. Thus, the effective damping approximation eq 5.14 for $J(\omega)$ has a much wider range of validity than would at first be apparent.

We checked the validity of eq 5.14 against the full calculation using eq 5.11 over the range of parameters described above. For the example presented in Figure 2 the difference between the two results lies within the thickness of the line. For example, for $\beta/\delta = 10^{-5}$, $M = 3$, or 6, and $s' < 4.5$ the greatest difference between the two expressions is less than 1%. Even for a more extreme, and physically nonsensical, example, $\beta/\delta = 10^{-3}$, $M = 1$, and $s' = 10^{6}$ the greatest discrepancy is only around 15%. It should be noted that if one must use a sum over a fractional number of bands the cancellation described above will not be as good. However, due to the extremely small difference between the results given by the two calculations and the inaccuracies inherent in any experimental fitting procedure, this should not cause any problems. Thus, it is clear that over any experimentally accessible region of parameter space, the effective damping expression, eq 5.14, can be used with confidence to incorporate the effect of side chains on the power spectrum.

To test the predictions of the present theory two kinds of complementary experimental studies are required. First, the relaxation properties of a homologous series of polymers in which a given side chain is attached at periodic intervals of increasing length, i.e., a, $2a$, $3a$, etc., should be measured. As indicated in the above discussion, the effective side chain damping constant should scale as $2\epsilon\delta^{1/2}/M\pi$ where M is the ratio of the repeat distance to the length of the minimum motional unit.[6] Furthermore, when M is increased, this series of experiments might also provide an estimate of the effective damping length of the local main chain dynamics. (In limit $M \to \infty$, the relaxation spectrum reduces to that of the polymer lacking any side chains.) Second, the local relaxation properties of polymers containing different side chains appended to the main chain at fixed a should be examined. By study of the chemically different main chains having the same side chain and extraction of the ϵ appropriate to the side chain, it would be of interest to examine the dependence of ϵ on the specific nature of the polymer backbone.

6. Summary and Conclusions

In this work we have extended our complex damped orientational diffusion model[3] of local, main chain dynamics to include the effects of inhomogeneities such as isolated attached probes and periodic side chains. We have done this within the context of the orientational diffusion model by treating the effect of a localized inhomogeneity as a local enhancement of the damping represented by a δ-function term in the diffusion equation. This enabled us to obtain expressions for the autocorrelation function and the power spectrum.

For isolated probes, such as are used in fluorescence and spin-labels, one is now able both to verify whether the probe exerts a minor perturbation on the local main chain dynamics and to disentangle the effects of the probe from the desired local main chain dynamics by fitting the experimental relaxation data to the expression including the probe-dependent strength parameter. To our knowledge this is the first time a method for doing this has been proposed.

For the case where the polymer has a periodic array of side chains attached to the main chain, it has been shown that for physically reasonable values of the side chain coupling parameter (and in fact even for physically unreasonable values of the parameter) the effect of the side chains is to modify the damping constant. Hence, what will be seen is the same main chain diffusional motion as the polymer chain would have in the absence of the side chains except that the damping constant is increased by the presence of the side chains. This means that even in the presence of side chains the more laborious procedure undertaken in section 5 need never be done in order to fit relaxation experiments, and the analytically solvable expressions for main chain dynamics previously presented can and should be used. We view this reduction of the problem of polymers with side chains to the previously solved case of polymers without side chains as the major new result of this work.

Finally, it has become increasingly apparent that experimental relaxation data on polymers can be fitted quite well by a variety of diffusional type models (see, e.g., the detailed comparison in the recent paper by Viovy, Monnerie, and Brochon[5]). These models are all quite similar in that they treat the local chain dynamics by using a hydrodynamic, diffusional approach. They differ in detail principally in the way they treat the short distance motion on the level of an orienting unit and to some extent in how they treat the longer distance hydrodynamic damping. Previously we have shown that the results are invariant to the details of how the damping is introduced.[1,8] Here (see discussion following eq 3.12) we have shown that the results are largely invariant to the details of how the short distance motion is treated. This is not surprising since the very use of a hydrodynamic diffusional picture implies that the short distance motion can be treated in an "averaged" manner. This invariance to the details of the models at long and short distances implies a certain robustness in the basic diffusion picture of orientational diffusion in polymer chains. This and the goodness of the fit of these models to experiments are gratifying from a theoretical point of view since they imply that this relatively simple picture adequately describes the relaxation spectrum of polymer chains. From the standpoint of those experimentalists who held the now rapidly dimming hope that relaxation experiments could illuminate the local molecular details of polymer motion, these conclusions are perhaps not as gratifying.

Acknowledgment is made to the donors of the Petroleum Research Fund, administered by the American Chemical Society, for partial support of this research. This work was also supported in part by a grant from the Polymers Program of the National Science Foundation (No. DMR-8303197). We also thank Dr. Dennis Perchak and Professor A. E. Carlsson for helpful discussions.

References and Notes

(1) (a) Skolnick, J.; Yaris, R. *Macromolecules* **1982**, *15*, 1041. (b) Skolnick, J.; Yaris, R. *Macromolecules* **1983**, *16*, 491.
(2) (a) Skolnick, J.; Yaris, R. *Macromolecules* **1982**, *15*, 1046. (b) Skolnick, J.; Yaris, R. *Macromolecules*, **1983**, *16*, 492.
(3) Skolnick, J.; Yaris, R. *Macromolecules* **1983**, *16*, 266.
(4) Skolnick, J.; Perchak, D.; Yaris, R. *J. Magn. Reson.* **1984**, *57*, 204.
(5) Viovy, J.; Monnerie, L.; Brochon, J. *Macromolecules* **1983**, *16*, 1845.
(6) Skolnick, J.; Mattice, W. L. *Macromolecules* **1981**, *14*, 292.
(7) Valeur, B.; Jarry, J. P.; Gény, F.; Monnerie, L. *J. Polym. Sci. Polym. Phys. Ed.* **1975**, *13*, 667, 675, 2251.
(8) Bendler, J.; Yaris, R. *Macromolecules* **1978**, *11*, 650.
(9) Gottfried, K. "Quantum Mechanics"; W. A. Benjamin Inc.: New York, 1966; Vol. I.
(10) Kronig, R.; Penney, W. G. *Proc. R. Soc. London, Ser. A* **1931**, *130*, 499.
(11) Saxon, D. S.; Hunter, R. A. *Philips Res. Rep.* **1949**, *4*, 81.
(12) Kittel, C. "Introduction to Solid State Physics", 5th ed.; Wiley: New York, 1976.
(13) Ashcroft, N. W.; Mermin, N. D. "Solid State Physics"; Holt, Rinehart and Winston: New York, 1976.